LETTERS

A spindle-independent cleavage furrow positioning pathway

Clemens Cabernard[1,2,3], Kenneth E. Prehoda[2] & Chris Q. Doe[1,2,3]

The mitotic spindle determines the cleavage furrow site during metazoan cell division[1,2], but whether other mechanisms exist remains unknown. Here we identify a spindle-independent mechanism for cleavage furrow positioning in *Drosophila* neuroblasts. We show that early and late furrow proteins (Pavarotti, Anillin, and Myosin) are localized to the neuroblast basal cortex at anaphase onset by a Pins cortical polarity pathway, and can induce a basally displaced furrow even in the complete absence of a mitotic spindle. Rotation or displacement of the spindle results in two furrows: an early polarity-induced basal furrow and a later spindle-induced furrow. This spindle-independent cleavage furrow mechanism may be relevant to other highly polarized mitotic cells, such as mammalian neural progenitors.

Elegant physical or genetic manipulations of the mitotic spindle have shown that the spindle determines the position of the cleavage furrow in a wide range of cells[1,2]. Although this is a common mechanism for furrow formation, it may not be the only one, as cleavage-furrow position during the highly asymmetric mammalian meiotic divisions can be specified by a spindle-independent chromosomal cue[3]. The spindle pathway for furrow positioning is initiated at the overlapping microtubules of the central spindle, where the 'centralspindlin' protein complex is assembled. Centralspindlin components include the kinesin Pavarotti (Zen-4 in *Caenorhabditis elegans*), the RACGAP50 Tumbleweed (Cyk-4 in *C. elegans*) and the RhoGEF Pebble (Ect-2 in *C. elegans*)[1,4]. After assembly, the centralspindlin complex moves to the cell cortex, possibly through a special population of stable microtubules[5], to form a cortical ring at the site of the central spindle. The centralspindlin ring subsequently recruits actomyosin and initiates cleavage furrow constriction. In contrast, astral microtubules typically inhibit furrow formation[4] (Fig. 1a, left).

Here we test whether the spindle-induced furrow model is sufficient to account for cleavage furrow positioning during asymmetric cell division of *Drosophila* neuroblasts. Neuroblasts establish molecular asymmetry during early prophase with the apical cortical localization of the Par complex (Bazooka; Par-6; atypical protein kinase C, aPKC) and the Pins complex (Partner of Inscuteable (Pins); Gαi; Discs large (Dlg))[6]. Subsequently, the scaffolding protein Miranda (Mira) and its cargo proteins Prospero (Pros), Brain tumour (Brat) and Staufen are localized to the basal cortex[6]. The mitotic spindle aligns along the apical/basal axis at metaphase and becomes asymmetric during anaphase, with the apical half forming longer astral and central spindle microtubules[7,8]. The cleavage furrow is displaced basally, generating a larger apical daughter cell and a smaller basal daughter cell. It has been assumed that the centralspindlin complex is the only mechanism for furrow positioning, because the furrow is always positioned adjacent to the central spindle, even in mutants that disrupt spindle asymmetry[8–13]. One model is that the basal spindle pole is anchored at the basal cortex, resulting in a basal displacement of the central spindle and subsequent cleavage furrow[11] (Fig. 1a, right). However, in neuroblasts, experiments such as spindle rotation, spindle displacement or spindle ablation have never been performed to test directly

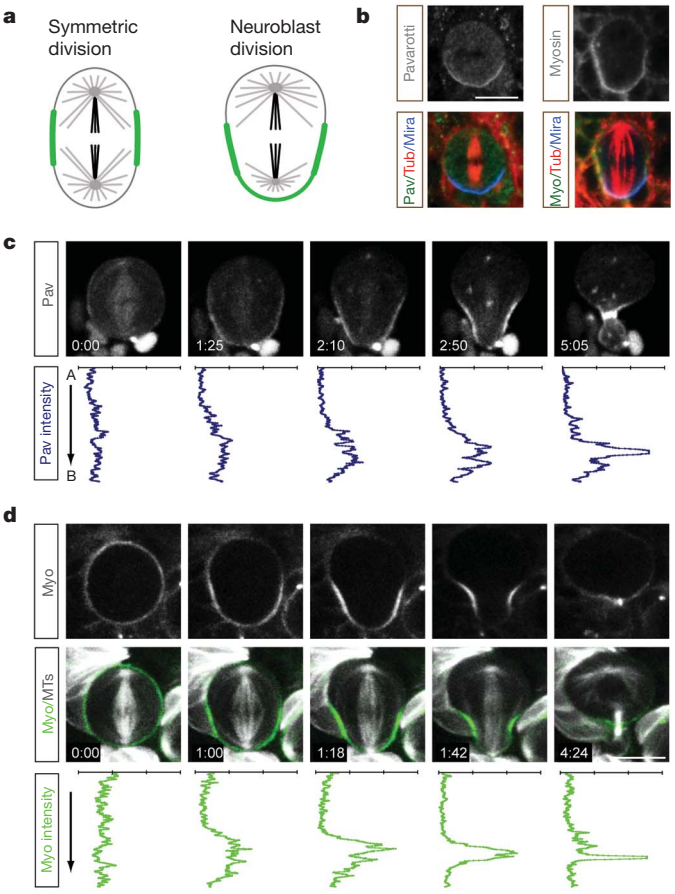

Figure 1 | Polarized cortical localization of Pav/Myosin furrow markers. **a**, Summary of cortical Pav/Myosin (green) localization during a representative symmetric cell division (left) or a neuroblast asymmetric cell division (right). Black, central spindle microtubules; grey, astral microtubules. **b**, Basal cortical localization of endogenous Pav/Myosin proteins in mitotic neuroblasts. **c**, **d**, Localization of Pav:GFP and Sqh:GFP (Myosin) from Supplementary Movies 1–3. Overlay is shown below single-channel image sequence. Bottom rows show plots of cortical pixel intensity for each protein around one half of the neuroblast cortex, from apical centre (top) to basal centre (bottom) of cortex. Apical up, basal down. Myo, Myosin, MTs, microtubules. Scale bars, 10 μm. Time is shown as minutes:seconds from anaphase onset.

[1]Howard Hughes Medical Institute, University of Oregon, Eugene, Oregon 97403, USA. [2]Institute of Molecular Biology, University of Oregon, Eugene, Oregon 97403, USA. [3]Institute of Neuroscience, University of Oregon, Eugene, Oregon 97403, USA.

whether the centralspindlin pathway is the sole mechanism for furrow positioning.

We began our investigation of neuroblast cleavage furrow positioning by assaying the timing and localization of three furrow components: the early furrow marker Pavarotti (Pav), an essential centralspindlin component[4]; Anillin, an early furrow component[14]; and Myosin regulatory light chain (called Myosin hereafter, encoded by the *sqh* gene), which is an essential component of the contractile ring. In symmetrically dividing cells, Pav/Anillin/Myosin are uniformly cortical at metaphase, and become progressively restricted to a cortical ring adjacent to the central spindle[15] (Fig. 1a, left). In neuroblasts, Pav/Anillin/Myosin proteins were uniformly cortical at metaphase and enriched at the furrow during anaphase–telophase; in addition, we saw asymmetric localization of Pav/Anillin/Myosin to the basal cortex of the neuroblast during early anaphase (Fig. 1b, Supplementary Fig. 1 and data not shown). The same localization was also observed by live imaging with Pav: green fluorescent protein (GFP)[16], Anillin:GFP[17] or Sqh:GFP[18] (Myosin) reporter proteins (Fig. 1c, d and Supplementary Movies 1–3; summarized in Fig. 1a, right). Measurements of pixel intensity further revealed that the basal enrichment of Pav:GFP, Anillin:GFP and Sqh:GFP (Myosin) is not uniform; all markers clear from the apical cortex first, followed by partial depletion from the basal tip, before accumulation in a basally shifted lateral position (Fig. 1c, d and data not shown). Our data differ slightly from previous work showing apical Sqh:GFP localization in prophase neuroblasts[19]; our Sqh:GFP live imaging showed fluctuating weak apical or basal cortical localization during prophase ($n = 10$; data not shown). Asymmetric basal enrichment of Pav/Myosin proteins was detectable 10–20 s before astral microtubule asymmetry, and over 40 s before central spindle asymmetry (Supplementary Fig. 2). Pav/Anillin/Myosin asymmetric cortical localization precedes spindle asymmetry, and thus is not easily explained by a spindle-induced furrow positioning model.

We next tested the role of the mitotic spindle in generating Pav/Myosin basal cortical localization and basal furrow positioning. First, we tested whether spindle astral microtubules were required to generate Myosin cortical asymmetry. *Sas-4* mutant neuroblasts lack centrioles, centrosomes and all astral microtubules, and were reported to undergo essentially normal asymmetric cell division[10], as do other mutants that lack spindle-pole asymmetry[11,13,20,21]. However, the localization of furrow proteins and the nature of the furrow positioning cue in these mutants has not been addressed. We found that *Sas-4* mutant neuroblasts established normal basal cortical localization of Myosin and basal furrow formation (Fig. 2a), and thus astral microtubules are not required for Myosin basal cortical localization or basal cleavage furrow positioning.

We next tested whether central spindle microtubules were required to generate Myosin cortical asymmetry and basal furrow formation. We performed live imaging of neuroblasts in which all microtubules were ablated by colcemid treatment, and a mutation in *rough deal* (*rod*) was used to bypass the metaphase-arrest checkpoint[22]. Surprisingly, all colcemid-treated *rod* mutant neuroblasts showed robust basal localization of Myosin and generated a basally displaced cleavage furrow, despite lack of any detectable microtubules (Fig. 2b and Supplementary Movie 4). Thus complete loss of microtubules does not affect basal furrow positioning. This is not a non-specific effect of microtubule loss, because most wild-type neuroblasts treated with colcemid are metaphase-arrested, maintain uniform cortical Myosin, and have no furrows (Fig. 2c). Furthermore, *rod* single mutants localize Myosin in an asymmetric fashion like wild-type neuroblasts (Supplementary Fig. 3). We conclude that neuroblasts have a spindle-independent mechanism for basal cleavage furrow positioning, and that activating this mechanism requires anaphase onset. We call this the 'polarity-induced' pathway because it is generated by neuroblast cortical polarity cues (see below).

Wild-type neuroblasts may use both spindle-induced and polarity-induced furrow positioning pathways, or just one of these pathways. To test whether both pathways are active in neuroblasts, we rotated or displaced the mitotic spindle within the neuroblast, and assayed for the ability of each pathway to specify furrow position. We performed spindle displacement experiments by examining the minority of colcemid-treated *rod* mutant neuroblasts where one or more tiny spindles form near the apical cortex. In these neuroblasts, we observed normal asymmetric basal localization of Myosin and basal furrow formation; slightly later we detected a second furrow adjacent to the small apical mitotic spindle (Fig. 3a, b and Supplementary Movie 5). Next, we performed spindle rotation experiments using the *mushroom body defective* (*mud*) mutant. In *mud* mutants approximately 15% of the spindles are orthogonal to the normal apical/basal polarity axis[23–25], thereby mimicking the physical spindle rotation experiments possible in larger cells[1,2]. We observed that *mud* mutant neuroblasts with the spindle orthogonal to the apical/basal polarity axis showed basal cortical localization of Pav/Anillin/Myosin and initiated a basal furrow (Fig. 3c, Supplementary Movies 6 and 7 and data not shown) that often pinched off an anucleate basal 'polar lobe' (Fig. 3d, Supplementary Fig. 4a and Supplementary Movie 8). Interestingly, basal-furrow initiation always preceded the spindle-induced furrow initiation (Fig. 3e and Supplementary Movie 9). Identical findings were observed in three other mutants that show neuroblast spindle rotation (*asterless*, *centrosomin* and *Sas-4*; Supplementary Fig. 4b). In both spindle displacement and spindle rotation experiments, the position of the mitotic spindle is uncoupled from the cortical polarity axis, and this allows us to observe cleavage furrows formed in response to each pathway. These experiments show that neuroblasts have two distinct furrow positioning pathways: a polarity-induced pathway and a spindle-induced pathway. In wild-type neuroblasts, both pathways promote basal furrow positioning, but spindle rotation/displacement experiments allow us to separate each pathway spatially and temporally (discussed below).

What is the molecular mechanism of the polarity-induced furrow pathway? We tested the centralspindlin core component Pav, as well

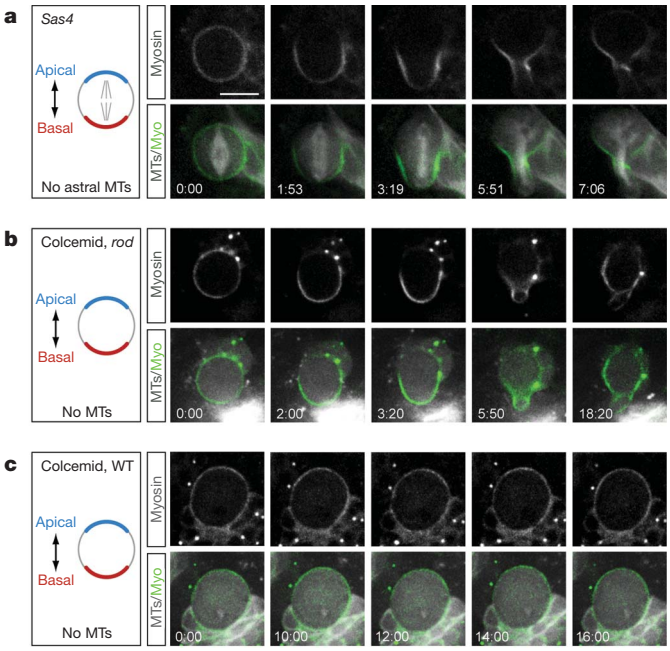

Figure 2 | Spindle-independent cleavage furrow positioning. **a**, Sas-4 mutant neuroblast lacks astral microtubules, yet still establishes basal Myosin localization and basal furrow position (100%, $n = 158$). **b**, Colcemid-treated *rod* mutant neuroblast lacks all spindle microtubules, yet still establishes basal Myosin localization and basal furrow position (100%, $n = 7$). **c**, Colcemid-treated wild-type neuroblast lacks all spindle microtubules, remains arrested at metaphase and does not establish basal Myosin localization or initiate furrow formation (100%, $n = 7$). A schematic of each experiment is shown to the left (blue/red, apical/basal polarity; grey, microtubules). All genotypes imaged in brains from late second or early third larval instars. Scale bars, 10 μm. Time is shown as minutes:seconds.

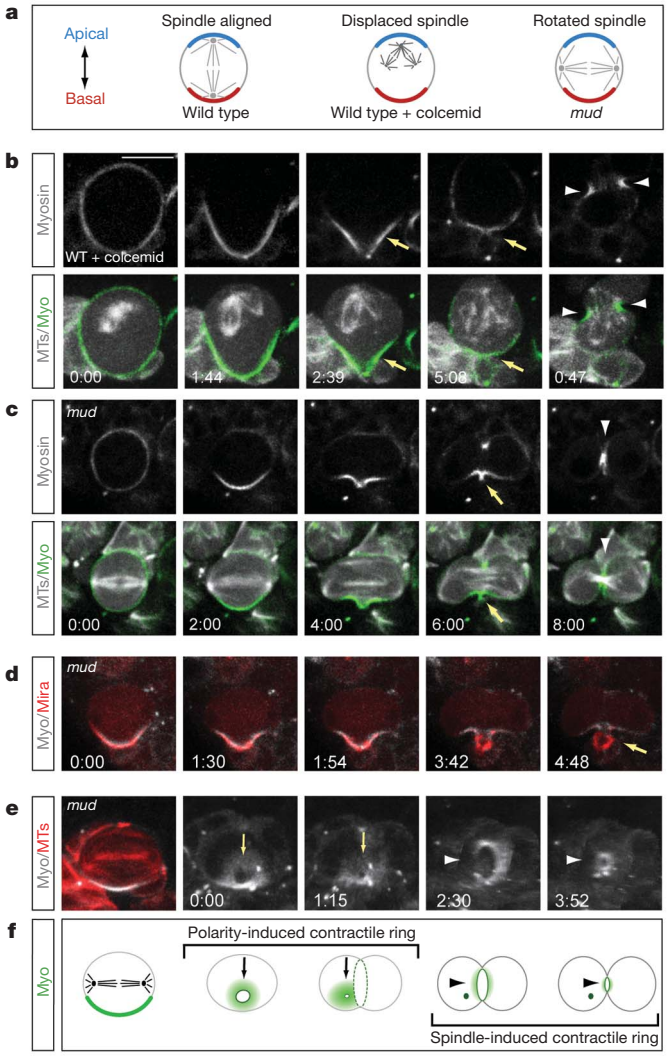

Figure 3 | Neuroblasts use both spindle-induced and polarity-induced furrow positioning pathways. **a**, Schematic of experimental design. Blue/red, apical/basal polarity; grey, spindle. **b**, Spindle displacement experiment: colcemid-treated neuroblasts with tiny apical spindles form two spatiotemporally distinct furrows: early basal furrow (arrow); later spindle-associated furrow (arrowhead). **c**–**f**, Spindle rotation experiment: *mud* mutant neuroblasts with spindles orthogonal to the apical–basal polarity axis form two spatiotemporally distinct furrows. **c**, Neuroblast forms an early basal furrow (arrow), followed by an orthogonal spindle-associated furrow (arrowhead). **d**, Neuroblast forms an early basal furrow that pinches off an anucleate 'polar lobe' (arrow). Cherry:Miranda marks the basal cortex. **e**, Still pictures from Supplementary Movie 9 showing the basal contractile ring 'en face' to document the progressive constriction of the contractile ring. Yellow arrows, basal furrow; white arrows, orthogonal spindle-associated contractile ring. **f**, Summary of spindle rotation experiment. Green, Myosin; black, spindle; green dot, midbody remnant. Time is shown as minutes:seconds. Scale bar, 10 μm.

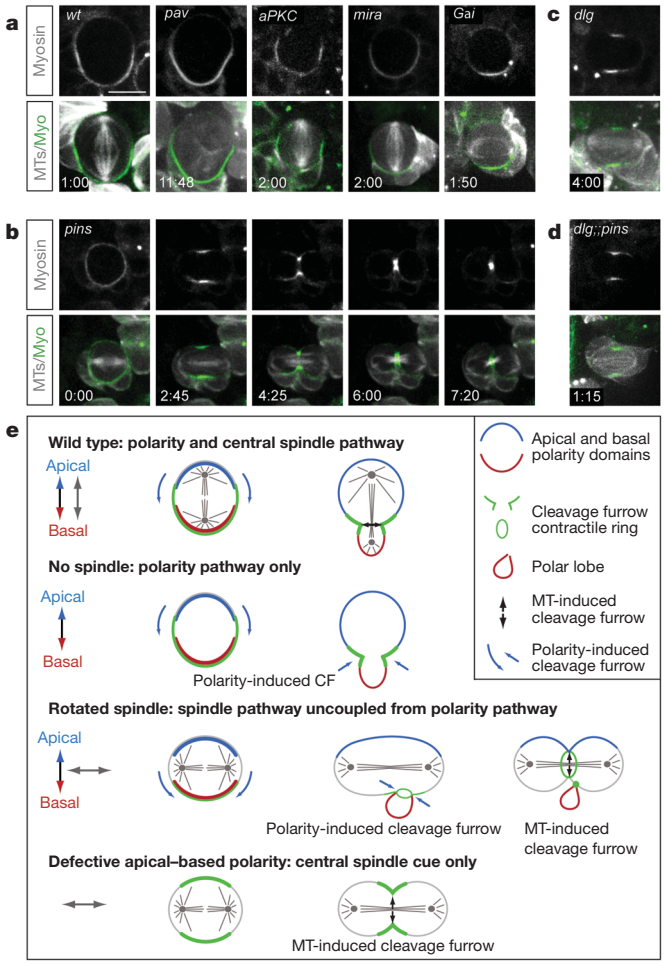

Figure 4 | Mechanism of polarity-induced furrow formation. **a**, Basal Myosin localization in anaphase neuroblasts is normal in neuroblasts strongly depleted for Pavarotti (Pav), aPKC, Miranda (Mira; mosaic analysis with a repressible cell marker (MARCM) clones) or zygotic null Gαi mutants. Time is shown as minutes:seconds in all panels. Scale bar, 10 μm. **b**, Zygotic *pins* single mutant larval neuroblast undergoing a symmetric division and showing symmetric Myosin (Sqh:GFP) localization. **c**, Zygotic *dlg* single mutant anaphase larval neuroblast undergoing a symmetric division and showing symmetric Myosin (Sqh:GFP) localization. **d**, Zygotic *dlg;;pins* double mutant anaphase neuroblast in early third larval instar undergoing a symmetric division and showing symmetric Myosin (Sqh:GFP) localization. **e**, Summary.

as each of the three major cortical polarity protein complexes (apical Par/aPKC, basal Miranda and apical Pins). We used inducible *pav* RNA interference transgene to reduce strongly Pav protein levels specifically in neuroblasts. This resulted in phenotypes matching that of a *pav* null mutation: the neuroblasts were enlarged and polyploid owing to failure of cytokinesis, and Pav protein was undetectable by antibody staining (data not shown). Surprisingly, these Pav-depleted neuroblasts showed normal basal localization of Myosin at early anaphase, and initiated a transient basal furrow (Fig. 4a). We conclude that the canonical centralspindlin pathway is not required for basal furrow formation. The apical Par complex member aPKC is essential for proper localization of all known basal proteins[6], but it is not required for basal localization of Myosin (Fig. 4a). Similarly, the basal scaffolding protein Miranda is not required for Myosin basal localization (Fig. 4a).

The final known polarity complex we tested was the apical Pins complex. We scored *pins* zygotic mutant neuroblasts at late second or third larval instar; most formed an asymmetric spindle and divided asymmetrically (89%; $n = 147$) and thus could not be assayed for polarity-induced furrow positioning owing to the presence of the canonical spindle-induced furrow pathway. More informative were the approximately 11% of *pins* mutant neuroblasts that had a symmetric spindle and divided symmetrically; all of these neuroblasts lacked Pav/Myosin basal cortical enrichment, lacked basal furrows and never formed 'polar lobes' (100%, $n = 19$; Fig. 4b, Supplementary Movie 10 and data not shown). To increase the percentage of symmetrically dividing *pins* mutant neuroblasts, we combined *pins* with a mutation in *dlg*, which is required for normal spindle asymmetry[9]. We found that 100% of the *dlg;;pins* double mutant neuroblasts showed symmetric spindles, and they all lacked Myosin basal cortical enrichment and basally displaced furrows (100%, $n = 20$;

Fig. 4d). The lack of asymmetric Myosin localization in the *pins* and *dlg;;pins* mutant neuroblasts is due to the loss of Pins, not the symmetric spindle, because *mud* and *Gαi* mutant neuroblasts have symmetric spindles and still show basal Myosin localization and basal 'polar lobe' formation (Figs 3c and 4a, Supplementary Movie 11 and data not shown). Thus Pins is an essential component of the polarity-induced cleavage furrow pathway. To test if Dlg has a role in the polarity induced furrow pathway, we examined *dlg* single mutants. Only a small fraction had a symmetric spindle (6%, $n = 65$); of these neuroblasts, two exhibited basally enriched Myosin (data not show) and two showed symmetric cortical Myosin (Fig. 4c). This partial phenotype suggests that Dlg plays a role in furrow positioning, but that Pins is likely to act through at least one other protein to regulate cleavage furrow position. We conclude that Pins/Dlg are components of the spindle-independent cortical polarity-induced cleavage positioning mechanism.

We have shown that neuroblasts use two pathways for specifying the site of cleavage furrow position: the well-studied centralspindlin pathway and a new cortical polarity pathway. In neuroblasts these pathways appear to work partly redundantly: the polarity-induced pathway alone can give a basal furrow (for example, in colcemid-treated *rod* mutant neuroblasts), whereas the spindle alone can induce an equatorial furrow (for example, in *dlg;;pins* mutant neuroblasts) (summarized in Fig. 4e). Although neuroblasts normally use both pathways redundantly, other cell types may uncouple the polarity-induced and spindle-induced pathways. For example, molluscan embryos often create determinant-filled 'polar lobes' which form earlier and orthogonal to the spindle-induced furrow[26]. Mammalian embryonic neuroepithelial cells are highly elongated along their apical/basal axis and can initiate cleavage furrowing at their basal endfoot, far from the site of the apical mitotic spindle[27]. It will be interesting to see if a polarity-induced furrow pathway exists in mammalian neuroepithelial cells, as well as other polarized cell types.

METHODS SUMMARY

We used the mutant alleles $aPKC^{K06403}$, $mira^{zz178}$, $pins^{P89}$, dlg^{m52} mud^{4}, gai^{8}, cnn^{hk21}, $Sas\text{-}4^{M}$, asl^{2}, $rod^{H4.8}$, the *UAS-PavRNAi* line 46137 from the Vienna Drosophila RNAi Center (see Methods for full stock references). Previously described methods were used for drug treatment[28], live imaging[29] and antibody staining[29]. Detailed methods are available in the Supplementary Information. All neuroblasts were imaged were from central brains of second or third larval instars.

Full Methods and any associated references are available in the online version of the paper at www.nature.com/nature.

Received 19 December 2009; accepted 28 June 2010.

1. Oliferenko, S., Chew, T. G. & Balasubramanian, M. K. Positioning cytokinesis. *Genes Dev.* **23,** 660–674 (2009).
2. von Dassow, G. Concurrent cues for cytokinetic furrow induction in animal cells. *Trends Cell Biol.* **19,** 165–173 (2009).
3. Deng, M., Suraneni, P., Schultz, R. M. & Li, R. The Ran GTPase mediates chromatin signaling to control cortical polarity during polar body extrusion in mouse oocytes. *Dev. Cell* **12,** 301–308 (2007).
4. Somers, W. G. & Saint, R. A RhoGEF and Rho family GTPase-activating protein complex links the contractile ring to cortical microtubules at the onset of cytokinesis. *Dev. Cell* **4,** 29–39 (2003).
5. Foe, V. E. & von Dassow, G. Stable and dynamic microtubules coordinately shape the myosin activation zone during cytokinetic furrow formation. *J. Cell Biol.* **183,** 457–470 (2008).
6. Knoblich, J. A. Mechanisms of asymmetric stem cell division. *Cell* **132,** 583–597 (2008).
7. Cai, Y. *et al.* Apical complex genes control mitotic spindle geometry and relative size of daughter cells in *Drosophila* neuroblast and pI asymmetric divisions. *Cell* **112,** 51–62 (2003).
8. Fuse, N., Hisata, K., Katzen, A. L. & Matsuzaki, F. Heterotrimeric G proteins regulate daughter cell size asymmetry in *Drosophila* neuroblast divisions. *Curr. Biol.* **13,** 947–954 (2003).
9. Albertson, R. & Doe, C. Q. Dlg, Scrib and Lgl regulate neuroblast cell size and mitotic spindle asymmetry. *Nature Cell Biol.* **5,** 166–170 (2003).
10. Basto, R. *et al.* Flies without centrioles. *Cell* **125,** 1375–1386 (2006).
11. Giansanti, M. G., Gatti, M. & Bonaccorsi, S. The role of centrosomes and astral microtubules during asymmetric division of *Drosophila* neuroblasts. *Development* **128,** 1137–1145 (2001).
12. Izumi, Y. *et al.* Differential functions of G protein and Baz-aPKC signaling pathways in *Drosophila* neuroblast asymmetric division. *J. Cell Biol.* **164,** 729–738 (2004).
13. Megraw, T. L., Kao, L. R. & Kaufman, T. C. Zygotic development without functional mitotic centrosomes. *Curr. Biol.* **11,** 116–120 (2001).
14. Field, C. M. & Alberts, B. M. Anillin, a contractile ring protein that cycles from the nucleus to the cell cortex. *J. Cell Biol.* **131,** 165–178 (1995).
15. Hickson, G. R., Echard, A. & O'Farrell, P. H. Rho-kinase controls cell shape changes during cytokinesis. *Curr. Biol.* **16,** 359–370 (2006).
16. Minestrini, G., Harley, A. S. & Glover, D. M. Localization of Pavarotti-KLP in living *Drosophila* embryos suggests roles in reorganizing the cortical cytoskeleton during the mitotic cycle. *Mol. Biol. Cell* **14,** 4028–4038 (2003).
17. Silverman-Gavrila, R. V., Hales, K. G. & Wilde, A. Anillin-mediated targeting of peanut to pseudocleavage furrows is regulated by the GTPase Ran. *Mol. Biol. Cell* **19,** 3735–3744 (2008).
18. Royou, A., Sullivan, W. & Karess, R. Cortical recruitment of nonmuscle myosin II in early syncytial *Drosophila* embryos: its role in nuclear axial expansion and its regulation by Cdc2 activity. *J. Cell Biol.* **158,** 127–137 (2002).
19. Barros, C. S., Phelps, C. B. & Brand, A. H. *Drosophila* nonmuscle myosin II promotes the asymmetric segregation of cell fate determinants by cortical exclusion rather than active transport. *Dev. Cell* **5,** 829–840 (2003).
20. Giansanti, M. G., Bucciarelli, E., Bonaccorsi, S. & Gatti, M. *Drosophila* SPD-2 is an essential centriole component required for PCM recruitment and astral-microtubule nucleation. *Curr. Biol.* **18,** 303–309 (2008).
21. Bonaccorsi, S., Giansanti, M. G. & Gatti, M. Spindle assembly in *Drosophila* neuroblasts and ganglion mother cells. *Nature Cell Biol.* **2,** 54–56 (2000).
22. Basto, R., Gomes, R. & Karess, R. E. Rough deal and Zw10 are required for the metaphase checkpoint in *Drosophila. Nature Cell Biol.* **2,** 939–943 (2000).
23. Bowman, S. K. *et al.* The *Drosophila* NuMA homolog Mud regulates spindle orientation in asymmetric cell division. *Dev. Cell* **10,** 731–742 (2006).
24. Izumi, Y. *et al. Drosophila* Pins-binding protein Mud regulates spindle-polarity coupling and centrosome organization. *Nature Cell Biol.* **8,** 586–593 (2006).
25. Siller, K. H., Cabernard, C. & Doe, C. Q. The NuMA-related Mud protein binds Pins and regulates spindle orientation in *Drosophila* neuroblasts. *Nature Cell Biol.* **8,** 594–600 (2006).
26. Conrad, G. W. & Williams, D. C. Polar lobe formation and cytokinesis in fertilized eggs of *Ilyanassa obsoleta*. I. Ultrastructure and effects of cytochalasin B and colchicine. *Dev. Biol.* **36,** 363–378 (1974).
27. Kosodo, Y. *et al.* Cytokinesis of neuroepithelial cells can divide their basal process before anaphase. *EMBO J.* **27,** 3151–3163 (2008).
28. Siegrist, S. E. & Doe, C. Q. Extrinsic cues orient the cell division axis in *Drosophila* embryonic neuroblasts. *Development* **133,** 529–536 (2006).
29. Cabernard, C. & Doe, C. Q. Apical/basal spindle orientation is required for neuroblast homeostasis and neuronal differentiation in *Drosophila. Dev. Cell* **17,** 134–141 (2009).

Supplementary Information is linked to the online version of the paper at www.nature.com/nature.

Acknowledgements We thank A. Brand, D. Glover, C.-Y. Lee, M. Peifer, J. Raff, E. Wieschaus, A. Wilde, and the Bloomington and Vienna Drosophila RNAi Center stock centres for fly stocks and/or antibody reagents; R. Andersen, B. Bowerman, M. Goulding and B. Nolan for comments on the manuscript; and T. Gillies and K. Hirono for technical support. This work was supported by the National Institutes of Health (GM068032; to K.P.), the American Heart Association (to C.C. and K.P.), the Swiss National Science Foundation (to C.C.) and HHMI (to C.Q.D.).

Author Contributions C.C., K.E.P. and C.Q.D. conceived and designed the project. C.C. performed all the experiments. C.C. and C.Q.D. wrote the manuscript with input from K.E.P.

Author Information Reprints and permissions information is available at www.nature.com/reprints. The authors declare no competing financial interests. Readers are welcome to comment on the online version of this article at www.nature.com/nature. Correspondence and requests for materials should be addressed to C.Q.D. (cdoe@uoregon.edu).

METHODS

Fly strains and genetics. All mutant chromosomes were balanced over Cyo, actin:GFP, TM3 actin:GFP, Ser, e or TM6B, Tb. We used Oregon R as wild type, and the following mutant chromosomes and fly strains: *aPKC*^{K06403} (ref. 30); *FRT82B mira*^{zz178} (ref. 31); *pins*^{P89} (flybase, *raps*^{P89}; ref. 32); *dlg*^{m52} (flybase, *dlg*^{14}; ref. 33); *mud*^{4} (ref. 34); *Gαi*^{8} (ref. 35); *cnn*^{hk21} (ref. 13); *FRT82B Sas-4*^{M} (ref. 10); *asl*^{2} (ref. 36); *rod*$^{H4.8}$ (ref. 22); *worGal4* (ref. 9); *worGal4, UAS-Cherry:Jupiter* (ref. 29); *worGal4, UAS-Cherry:Mira* (ref. 29); *anillin:GFP* (ref. 17); *baz:GFP* (ref. 37); *baz:GFP, mud*^{4} (ref. 29); *UAS-GFP:PavNLS5* (ref. 16); *Sqh:Cherry* (ref. 38); *Sqh:GFP* (ref. 18); *worGal4, UAS-GFP:Mira, UAS-cherry:Jupiter* (ref. 29); *UAS-PavRNAi*^{46137} (ref. 39).

Recombinant chromosomes. The following recombinant chromosomes were generated using standard genetic procedures: *worGal4, UAS-Cherry:Jupiter, Sqh:GFP* (this work); *worGal4, UAS-GFP:PavNLS5* (this work).

MARCM analysis. For generating Mira MARCM clones[40], we crossed the analysis line *hsFLP70/hsFLP70; worGal4, UAS-Cherry:Jupiter, Sqh:GFP, tubGal80 FRT82B/TM6C, Sb* (this work) to Mira *FRT82B mira*^{zz178} and heat-shocked the progeny 24–48 h after larval hatching for 1 h at 37 °C. For live imaging, *mira* mutant clones of third-instar larvae were used.

Pavarotti RNAi experiment. Pavarotti knockdown was achieved by crossing *worGal4* (ref. 9) driver line to *UAS-PavRNAi*^{46137} (ref. 39). Loss of Pavarotti was confirmed using the anti-Pav antibody[16].

Colcemid experiments. For colcemid experiments, the following strains were used: *+; worGal4, UAS-Cherry:Jupiter, Sqh:GFP* (this work) or *+; worGal4, UAS-Cherry:Jupiter, Sqh:GFP; rodH4.8* (this work).

Wild-type or *rod*$^{H4.8}$ mutant neuroblasts were incubated with colcemid in live imaging medium[29] at a final concentration of 0.1 μm ml^{-1}. Live imaging was started without delay. Mild spindle phenotypes became apparent immediately after colcemid exposure, whereas complete spindle depolymerization was seen approximately 30–60 min after colcemid addition.

Immunohistochemistry. The following antibodies were used for this study: guinea pig anti-Miranda (1:1,000), rabbit anti-Zipper (1:500; this work), rabbit anti-Pavarotti (1:500)[16], mouse anti-Tubulin DM1A (Sigma, 1:1,500), rat anti-Pins (1:300)[25] and rabbit anti-Gαi (1:500)[41]. Secondary antibodies were from Invitrogen/Molecular Probes.

Imaging, post-imaging procedures and measurements. Live imaging methods were previously described[29]. Fixed preparations were imaged on a Leica SP2, and for Supplementary Fig. 1a on a Leica SP5, confocal microscope. Live samples were imaged on a McBain spinning disc confocal microscope equipped with a Hamamatsu EM-CCD (electron-multiplying charge-coupled device) camera, using a ×63 1.4 numerical aperture oil-immersion objective. Pixel intensity measurements (Fig. 1c, d) were performed using ImageJ. Only one-half of the neuroblasts' cortex was measured starting at the apical cortex and ending at the basal cortex. Post-imaging processing and measurements were performed in ImageJ or Imaris 6.2–7.0 (Bitplane).

Larval staging. For all experiments, late second- or third-instar larvae were used for analysis.

30. Rolls, M. M. *et al. Drosophila* aPKC regulates cell polarity and cell proliferation in neuroblasts and epithelia. *J. Cell Biol.* **163,** 1089–1098 (2003).
31. Caussinus, E. & Gonzalez, C. Induction of tumor growth by altered stem-cell asymmetric division in *Drosophila melanogaster*. *Nature Genet.* **37,** 1125–1129 (2005).
32. Yu, F. *et al.* Analysis of partner of inscuteable, a novel player of *Drosophila* asymmetric divisions, reveals two distinct steps in inscuteable apical localization. *Cell* **100,** 399–409 (2000).
33. Woods, D. F. & Bryant, P. J. Molecular cloning of the lethal(1)discs large-1 oncogene of *Drosophila*. *Dev. Biol.* **134,** 222–235 (1989).
34. Guan, Z. *et al.* Mushroom body defect, a gene involved in the control of neuroblast proliferation in *Drosophila*, encodes a coiled-coil protein. *Proc. Natl Acad. Sci. USA* **97,** 8122–8127 (2000).
35. Yu, F. *et al.* Distinct roles of Gαi and Gβ13F subunits of the heterotrimeric G protein complex in the mediation of *Drosophila* neuroblast asymmetric divisions. *J. Cell Biol.* **162,** 623–633 (2003).
36. Bonaccorsi, S., Giansanti, M. G. & Gatti, M. Spindle self-organization and cytokinesis during male meiosis in asterless mutants of *Drosophila melanogaster*. *J. Cell Biol.* **142,** 751–761 (1998).
37. Buszczak, M. *et al.* The Carnegie Protein Trap Library: a versatile tool for *Drosophila* developmental studies. *Genetics* **175,** 1505–1531 (2007).
38. Martin, A. C., Kaschube, M. & Wieschaus, E. F. Pulsed contractions of an actin-myosin network drive apical constriction. *Nature* **457,** 495–499 (2009).
39. Dietzl, G. *et al.* A genome-wide transgenic RNAi library for conditional gene inactivation in *Drosophila*. *Nature* **448,** 151–156 (2007).
40. Lee, T. & Luo, L. Mosaic analysis with a repressible cell marker for studies of gene function in neuronal morphogenesis. *Neuron* **22,** 451–461 (1999).
41. Siegrist, S. E. & Doe, C. Q. Microtubule-induced Pins/Gαi cortical polarity in *Drosophila* neuroblasts. *Cell* **123,** 1323–1335 (2005).